[2] Kidd, E. A., Bull, G., and Harper, R. P., Jr., "In-flight simulation—theory and application," AGARD Rept. 368 (April 1961).
[3] Chalk, C. R., "Additional flight evaluations of various longitudinal handling qualities in a variable-stability jet fighter," Wright Air Development Center WADC TR 57-719, Part II (1958).
[4] McFadden, N. M., Vomaske, R. F., and Heinle, D. R., "Flight investigation using variable-stability airplanes of minimum stability requirements for high-speed, high-altitude vehicles," NASA TN D-779 (1961).
[5] Bull, G., "A flight investigation of acceptable roll to yaw ratio of the Dutch roll, and acceptable spiral divergence," Cornell Aeronautical Lab. Rept. TB-574-F-6 (February 12, 1952).
[6] Liddell, C. J., Jr., Creer, B. Y., and Van Dyke, R. D., Jr., "A flight study of requirements for satisfactory lateral oscillatory characteristics of fighter aircraft," NACA RM A51E16 (1951).
[7] Harper, R. P., Jr., "In-flight simulation of the lateral-directional handling qualities of entry vehicles," Wright Air Development Center WADC TR 61-147 (November 1961).
[8] Petersen, F. S., Rediess, H. A., and Weil, J., "Lateral-directional control characteristics of the X-15 airplane," NASA TM X-726 (1961).
[9] McNeill, W. E. and Creer, B. Y., "A summary of results obtained during flight simulation of several aircraft prototypes with variable-stability airplanes," NACA RM A56C08 (1956).
[10] Breuhaus, W. O., "Dry-run in the 'X-15'," Research Trends IX, Cornell Aeronaut. Lab., 1-4 (1961).
[11] Gould, D. G., "The model controlled method for development of variable stability aircraft," Natl. Research Council of Canada Aeronautical Rept. LR-345 (June 1962).
[12] Ashkenas, I. L. and McRuer, D. T., "A theory of handling qualities derived from pilot-vehicle system considerations," Aeronaut. Eng. 21, 60–61, 83–102 (February 1962).

JULY-AUGUST 1964 J. AIRCRAFT VOL. 1, NO. 4

Prediction of Flutter Onset Speed Based on Flight Testing at Subcritical Speeds

NORMAN H. ZIMMERMAN* AND JASON T. WEISSENBURGER†
McDonnell Aircraft Corporation, St. Louis, Mo.

The commonly employed damping vs velocity technique of flight flutter testing is known to have a number of shortcomings which adversely affect the reliability and safety of such testing. The damping measurements in themselves give little useful information beyond stating whether or not flutter was encountered at the test speeds flown; magnitude of the damping has all too frequently been a grossly misleading indication of flutter stability margin. A new technique of flight flutter testing is presented herein based on the use of a flutter stability parameter truly indicative of the state of flutter stability within the system. This flutter stability parameter is based on measured frequency and decay data taken during flight and clearly shows the erosion of flutter margin with increasing speed. Using this information, together with a flutter prediction technique also presented herein, it is possible to predict the behavior of the flutter margin at speeds not yet flown and to predict the speed of flutter onset. The analytical considerations leading to the technique are developed, followed by experimental evidence substantiating this approach.

Nomenclature

$a_{1,2,3}$ = coefficients arising in equation for lift forces, Eq. (A3)
$A_{0,1,2,3}$ = coefficients of characteristic equation
$b_{1,2,3}$ = coefficients arising in equation for aerodynamic moment, Eq. (A3)
$B_{0,1,2}$ = coefficients in prediction equation
$C_{L\alpha}$ = lift curve slope
f = flutter (subscript)
F = flutter margin
h = translational displacement of center of gravity, Fig. 3
I_c = moment of inertia of airfoil about center of gravity
k_α = torsion spring constant
k_h = bending spring constant
L = aerodynamic lift
m = mass of airfoil
M_c = aerodynamic moment referred to center of gravity
P = operator, d/dt
q = dynamic pressure = $\frac{1}{2}\rho V^2$
s = complex root of characteristic equation
V = velocity (airspeed)
x = distance of center of gravity aft of elastic axis
α = torsional displacement of airfoil
β = real part of solution of characteristic equation i.e., negative of decay rate
ω = imaginary part of solution of characteristic equation, i.e., frequency

Presented at the AIAA/AFFTC/NASA-FRC Conference on Testing of Manned Flight Systems, Edwards Air Force Base, Calif., December 4–6, 1963 (no preprint number; published in bound volume of preprints of the meeting); revision received May 18, 1964.

* Scientist. Associate Fellow Member AIAA.
† Senior Dynamics Engineer. Member AIAA.

Introduction

Background

THOSE who have been involved in flight flutter test programs are well aware of its hazardous nature and the difficulties of obtaining meaningful data. The damping vs velocity technique that is commonly employed presents definite hazards, such as the decision to proceed to higher speeds based on extrapolating the data obtained up to the last test speed. Uncertainties connected with the technique of extrapolation are further compounded by scatter in the measured damping data upon which the extrapolation is based, even if due care is exercised. Extreme dangers are particularly inherent for configurations prone to sudden and violent flutter, i.e., abrupt damping degradation with no prior warning.

These observations are shown more dramatically in Fig. 1 where velocity-damping trends are shown for three different

configurations: one prone to mild flutter, one prone to moderate flutter, and one prone to explosive (sudden and violent) flutter. In all these cases, damping initially increases until some speed V_a is reached; above this speed, damping decreases until flutter occurs. In the case of mild flutter, damping degradation above V_a is gradual, and (with good measured data) the trend toward impending flutter would probably be apparent in flight testing. On the other hand, for explosive flutter, damping degradation above V_a is abrupt with hardly any prior warning, just the opposite of that which would be desirable.

The logic behind the extensive use of the velocity-damping technique probably stems from the very basic notion that the system is stable when damping is positive and unstable when damping is negative; therefore, why not monitor the damping during flight testing for indications of an approaching flutter? The potential dangers in this approach have already been shown, and experienced engineers in this field are well aware of them. Thus the real problem here is to find other practical flight test techniques which avoid the deficiencies of the velocity-damping technique.

New Slant on the Problem

In seeking a more meaningful and safer flight flutter test approach, it occurred to the authors that possibly the damping of in-flight vibrations is only a remote surface indication of something more fundamentally indicative of the stability processes going on within the system itself. Following up on this notion led to the stability criteria and technique presented in this paper. A brief description of this approach follows; it is covered more fully in subsequent sections.

A flutter stability parameter is defined which is indicative of the state of stability existing within the system for the corresponding airspeed. At any given airspeed it can be evaluated using only measured in-flight frequencies and decay rates. A plot of the variation of flutter stability parameter vs dynamic pressure is shown in Fig. 2 for a hypothetical but typical case. The circles would represent the

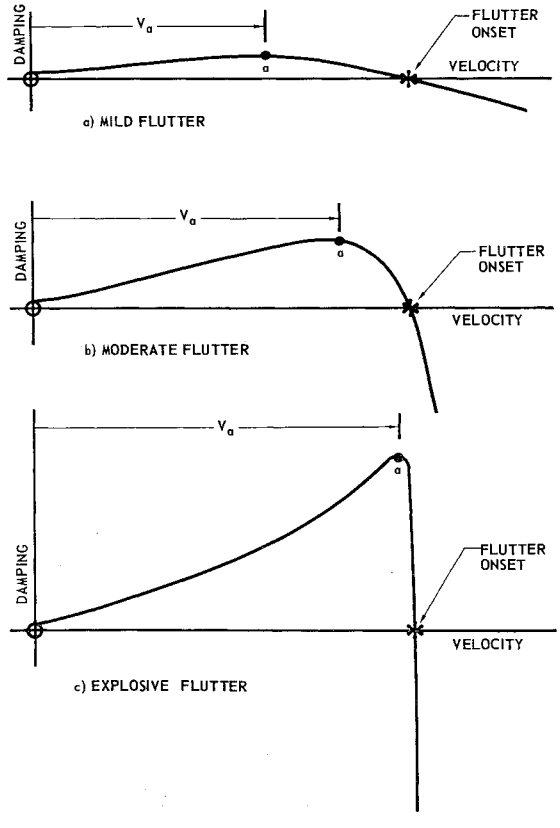

Fig. 1 Damping as an indication of flutter.

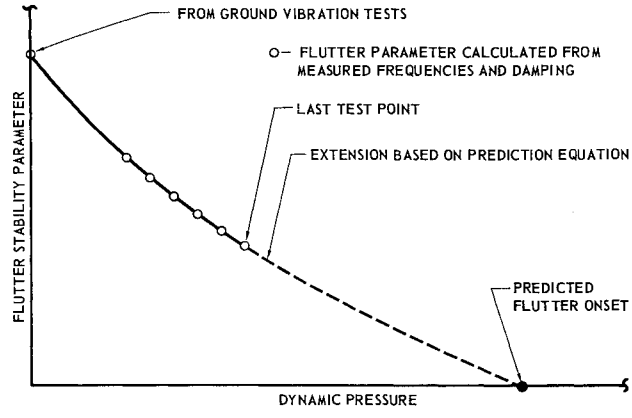

Fig. 2 Typical plot of stability parameter vs dynamic pressure.

flutter stability parameter computed from measured frequency and decay data at the corresponding speeds. This curve behaves in a civilized manner and is not prone to sudden or unexpected reversals, such as would be the case if damping alone were plotted. This is so, even for configurations prone to explosive flutter. The ordinate at any airspeed is a measure of the flutter stability remaining in the system and might more appropriately be thought of as the "flutter margin" for that speed. The smooth and continuous degradation of flutter margin with increasing speed is clearly evident. Moreover, disregarding effects usually of secondary influence, this curve will be shown to be a parabola whose coefficients can be evaluated from flight data taken up to the last test speed. This allows analytical extension of the curve beyond the last test point (shown dashed) and prediction of the flutter onset speed. In addition, the slope with which the extended curve crosses the abscissa is an indication of the predicted severity of the flutter. And, finally, this technique is particularly effective in providing early and unmistakable indications of the approach to an explosive flutter.

The technique presented in this paper is straightforward and simple to apply, requiring only data which might normally be obtained in flight flutter testing, i.e., frequencies and dampings. No knowledge of configuration details is necessary.

Scope of Paper

The authors hopefully intend that this paper will serve the following threefold purpose: 1) to present the salient concepts and developments embodied in introducing a new technique for use in flight flutter testing, i.e., to set forth a basic foundation upon which an entirely new and practical philosophy of flight flutter testing can be built; 2) to show that this basic foundation (which is developed in the main body of the paper) can be used as is without further refinements for practical flight flutter testing with good reliability over a broad range of applicability; 3) to suggest some possible refinements to the basic approach for increasing its range of applicability or degree of reliability. The content and organization of this paper have been arranged with the intent of achieving these objectives in a clear, concise, and straightforward manner.

The main body of this paper covers the salient features underlying the development and application of this new philosophy for flight flutter testing. In the interest of clarity here, the authors have taken the liberty of resorting to "poetic license" in a sense. Specifically, detailed effects normally of minor consequence have been purposely avoided while concentrating attention on the primary flutter-producing mechanism. (Refinements to the basic approach accounting for omitted detailed effects are subsequently covered in Appendix B, but limited experience to date indi-

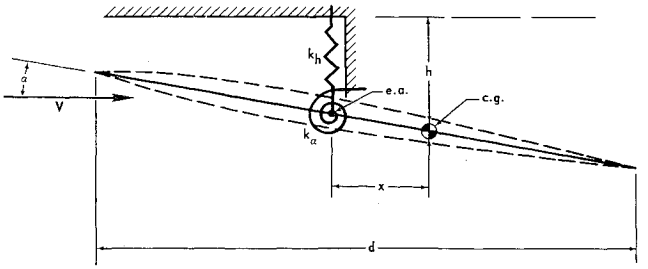

Fig. 3 Schematic of simple bending/torsion idealization.

cates that generally little is gained from these refinements.) In addition to developing the technique and its application for flight flutter testing, the main body also includes supporting experimental evidence, since analytical justification in itself is hardly sufficient to instill confidence in a new and different approach. For those desiring to delve further into details, Appendix A contains a detailed mathematical development of the technique, Appendix B discusses refinements that can be incorporated, and Appendix C introduces a very simple approximate technique that can be used for rapid, on-the-spot monitoring of flight flutter test programs.

The basic concepts and analytical development presented herein are based on a two-degree-of-freedom analysis. In a rigorous sense, then, it would appear that the technique would be of little practical value for the multi-degree-of-freedom systems encountered in practice. However, most cases of flutter, even for multi-degree-of-freedom systems, occur as a result of the interaction between only the two predominant system degrees-of-freedom. A more forceful argument emphasizing the practical value of the two-degree-of-freedom analysis lies in the good agreement with experimental results on practical multi-degree-of-freedom configurations. Extension of the technique to broaden its scope of applicability to configurations sometimes encountered which flutter as a result of interactions between more than two-degrees-of-freedom is possible, but this is outside the intended scope of the present paper.

Finally, in developing the theoretical foundation for the criteria and technique, concepts of common engineering familiarity are purposely employed so that engineers not necessarily specializing in flutter will find the development straightforward.

Development of the Technique

General

Only the highlights in the analytical development are covered here to avoid loss of continuity which might otherwise result from preoccupation with too many details. The analytical development covered here is based on a two-degree-of-freedom analysis. To enhance retention of physical significance in the development, the familiar bending/torsion idealization is employed; for the purpose at hand, a generalized two-degree-of-freedom idealization would yield the same results as can readily be verified.

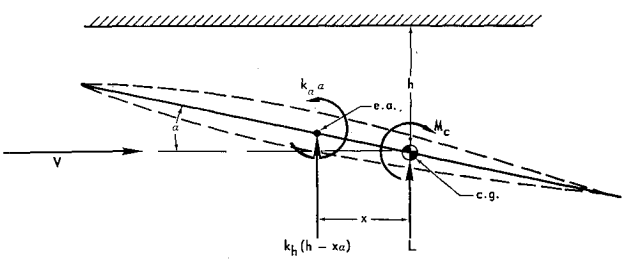

Fig. 4 Free body diagram for bending/torsion idealization.

Equations of Motion

The idealization is shown schematically in Fig. 3, and the corresponding free body diagram is shown in Fig. 4. In essence, the system possesses a translational inertia represented by m and a rotational inertia represented by I_c, and is subject to a translational elastic restraint k_h and a rotational elastic restraint k_α about the elastic axis. The aerodynamic forces acting on the system are referred to the center of gravity and consist of the lift force L and pitching moment M_c. All of the foregoing quantities represent spanwise weighted averages.

Summing the forces (positive down) and torques about the center of gravity (positive leading edge up), we have

$$\begin{aligned} m\ddot{h} &= -k_h(h - x\alpha) - L \\ I_c\ddot{\alpha} &= -k_\alpha\alpha + k_h(h - x\alpha)x + M_c \end{aligned} \tag{1}$$

The aerodynamic force and moment (referred to the center of gravity) are proportional in an over-all sense to the dynamic pressure q. These are further proportional to the angle of attack α, the plunging velocity $\dot{h}$, and the pitching velocity $\dot{\alpha}$. The aerodynamics will, therefore, be represented in the form

$$\begin{aligned} L &= C_{L_\alpha} q \left[a_1\alpha + a_2\left(\frac{\dot{h}}{V}\right) + a_3\left(\frac{\dot{\alpha}}{V}\right)\right] \\ M_c &= C_{L_\alpha} q \left[b_1\alpha + b_2\left(\frac{\dot{h}}{V}\right) + b_3\left(\frac{\dot{\alpha}}{V}\right)\right] \end{aligned} \tag{2}$$

where the proportionality constants a_1–b_3 reflect specific configuration geometry. The lift curve slope C_{L_α} has been factored out along with the dynamic pressure for subsequent convenience. Upon substituting Eqs. (2) into (1), there results a set of simultaneous linear differential equations (in the two unknowns α and h) with constant coefficients. The solution to such a set is well known and can be represented in the form

$$\begin{aligned} h &= h_0 e^{st} \\ \alpha &= \alpha_0 e^{st} \end{aligned} \tag{3}$$

where h_0 and α_0 are arbitrary integration constants and s represents the eigenvalues determined by substituting Eqs. (3) into the simultaneous differential equations. Upon substitution, there results the quartic characteristic equation in s,

$$s^4 + A_3s^3 + A_2s^2 + A_1s + A_0 = 0 \tag{4}$$

The coefficients A_0–A_3 are composites of the configuration constants and the product $C_{L_\alpha}q$, which reflects airspeed. Thus the coefficients in the characteristic equation would be expected to vary with airspeed.

Routh's Stability Criteria

In a rather direct manner, Routh's criteria for a system to be stable requires that all the coefficients of the characteristic equation be positive, and, furthermore, for the specific case of a quartic equation, the following relation must exist between the coefficients:

$$\left[A_2\left(\frac{A_1}{A_3}\right) - \left(\frac{A_1}{A_3}\right)^2 - A_0\right] > 0$$

or in somewhat modified form,

$$\left\{\left[\left(\frac{A_2}{2}\right)^2 - A_0\right] - \left[\frac{A_2}{2} - \frac{A_1}{A_3}\right]^2\right\} > 0 \tag{5}$$

Now from physical considerations alone we know that the system we are concerned with is stable at the lower speeds. Thus, all the A's must be initially positive and the inequality of Eq. (5) must be satisfied. Transition to an oscillatory instability (flutter) results when the inequality is reversed. In a physical sense then, for flutter testing we need only be concerned with the inequality of Eq. (5) and define as a flutter stability parameter the quantity

$$F = \left[\left(\frac{A_2}{2}\right)^2 - A_0\right] - \left[\frac{A_2}{2} - \frac{A_1}{A_3}\right]^2 \qquad (6)$$

which must be positive for stability to exist; the more positive, the greater the degree of stability. It is seen that the quantity F defined above is nothing more than a measure of system stability as expressed in the Routh criteria and is thus fundamentally indicative of the state of the stability processes going on within the system itself, in contrast to the remote surface indication embodied in the system damping. Since the A's vary with airspeed, the value of F will also be expected to depend upon airspeed. Its numerical value at any given speed may be thought of as the flutter stability margin yet remaining in the system for that speed. For that reason, we shall henceforth refer to F as the "flutter margin."

Evaluation of Flutter Margin from Flight Data

Let the four roots of the characteristic equation, Eq. (4), be designated by s_1, s_2, s_3, and s_4. These can be expressed in the complex form

$$s_{1,2} = \beta_1 \pm i\omega_1$$

$$s_{3,4} = \beta_2 \pm i\omega_2$$

where the ω's would represent the system frequencies and the β's would represent the negative of the system decay rates. The characteristic equation may thus be rewritten in the alternate form

$$(s - s_1)(s - s_2)(s - s_3)(s - s_4) = 0$$

$$[s - (\beta_1 + i\omega_1)][s - (\beta_1 - i\omega_1)] \times [s - (\beta_2 + i\omega_2)][s - (\beta_2 - i\omega_2)] = 0$$

Expanding this out and comparing like coefficients with Eq. (4), we can solve for the A's in terms of the β's and ω's. These in turn are introduced into Eq. (6), yielding for the flutter margin,

$$F = \left[\left(\frac{\omega_2^2 - \omega_1^2}{2}\right) + \left(\frac{\beta_2^2 - \beta_1^2}{2}\right)\right]^2 + 4\beta_1\beta_2\left[\left(\frac{\omega_2^2 + \omega_1^2}{2}\right) + 2\left(\frac{\beta_2 + \beta_1}{2}\right)^2\right] - \left[\left(\frac{\beta_2 - \beta_1}{\beta_2 + \beta_1}\right)\left(\frac{\omega_2^2 - \omega_1^2}{2}\right) + 2\left(\frac{\beta_2 + \beta_1}{2}\right)^2\right]^2 \qquad (7)$$

It is then possible, using Eq. (7), to evaluate the flutter margin corresponding to any selected airspeed simply by measuring the in-flight frequencies ω_1 and ω_2 and decays β_1 and β_2 for that airspeed using a flight resonance or other suitable technique. This would yield a set of data such as that shown by the open circles in Fig. 5.

Flutter Prediction Equation

In the previous section, it was shown how the flutter margin existing at any airspeed could be obtained from frequency and decay data measured at the corresponding speed. In other words, Eq. (7) allows one to observe the erosion of flutter margin with increasing airspeed but only up to the last test speed. It makes no commitment on what lies beyond. It is possible, however, to predict how the flutter margin will behave at speeds not yet flown from analytical considerations of the flutter mechanism. As in the previous section, we again use Eq. (6) which defines the flutter margin in a general sense, but now we shall obtain the A's entering therein from alternate considerations. If the steps leading to the characteristic equation, Eq. (4) are carried out, it will be seen that A_0 through A_3 are analytical functions of the specific configuration constants and the product $C_{L\alpha}q$. Now then, if these analytical expressions for A_0 through A_3 are introduced into Eq. (6), there results the alternate expression for the flutter margin

$$F = B_2(C_{L\alpha}q)^2 + B_1(C_{L\alpha}q) + B_0 \qquad (8)$$

where the configuration constants are embodied in the coefficients B_0, B_1, and B_2. Equation (8) will be called the "flutter prediction equation." Actually, it is not necessary to know anything about the configuration details for evaluation of the B's. A simpler and more powerful approach can be employed for this, as is shown in the next section.

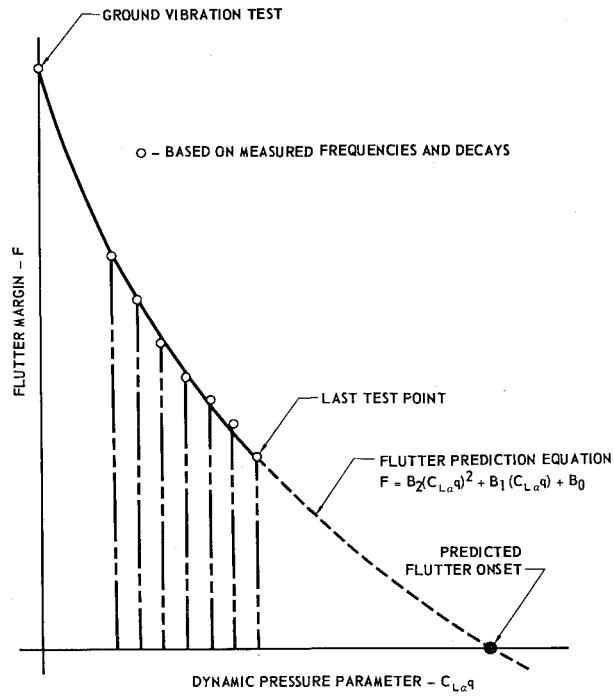

Fig. 5 Application of flutter margin technique.

Flutter Prediction Technique

Referring again to Fig. 5, let it be assumed that flight testing has progressed up to the speed corresponding to the last test point shown and that the flutter margins indicated by the open circles have been computed from the flight test data using Eq. (7). Now the flutter prediction equation indicates that the curve connecting these circles should be a parabola expressible by Eq. (8). Hence, the coefficients B_0, B_1, and B_2 are evaluated to yield a parabola best fitting the available data. (Data scatter and other influences discussed later may cause the curve to depart somewhat from a precise parabola.) Having thus evaluated the B coefficients using the prior flight test data, Eq. (8) can now be employed to predict how the flutter margin will behave at the speeds not yet flown. This is shown as the dashed extension of the solid curve passing through the test points in Fig. 5. Predicted flutter onset occurs when the predicted flutter margin diminishes to zero. The predicted severity of the flutter is indicated by the slope of the curve at zero flutter margin.

The Role of $C_{L\alpha}$

The lift curve slope $C_{L\alpha}$ was included along with the dynamic pressure q in the product $C_{L\alpha}q$ to allow for greater

diversity in application of the technique. For example, if flight testing encompasses the high subsonic as well as the low subsonic region, then C_{L_α} will tend to increase with the higher speeds. In spite of this variation in C_{L_α}, Eq. (8), the flutter prediction equation, still requires that a parabolic relationship exist between the flutter margin F and the product $C_{L_\alpha}q$. The advantages occurring from retaining the parabolic form, regardless of variations in C_{L_α}, should be apparent. A particularly convenient form of the flutter prediction equation results if C_{L_α} can be considered a constant. Equation (8) can then be written

$$F = (B_2C_{L_\alpha}{}^2)q^2 + (B_1C_{L_\alpha})q + B_0$$

$$F = B_2'q^2 + B_1'q + B_0$$

Upon dropping the unnecessary primes, we have

$$F = B_2q^2 + B_1q + B_0 \qquad (8a)$$

where again B_2, B_1, and B_0 are configuration constants. Thus, with constant C_{L_α}, the flutter margin varies parabolically with q only. Equation (8a) is nearly correct except for large variations of C_{L_α}.

One final clarifying remark appears appropriate in regard to the role of C_{L_α}. In a rigorous sense, C_{L_α} should properly include the effects of oscillatory aerodynamics, as well as steady flow aerodynamics. However, its inclusion has only a minor effect on the results and might more appropriately be classified as a refinement to the basic technique presented herein. At any rate, further discussion in regard to this is more appropriately a subject for Appendix B on refinements.

Comparison with Experiment

Although the analytical considerations employed in developing the technique might seem to make good sense, a more direct proof of its validity by comparison with experiment is appropriate. Three such comparisons are shown in this section while a fourth is shown in Appendix C where an unusually simple, approximate technique is discussed. Some idea of the versatility of the approach can be gained by considering that the four configurations used in these comparisons were quite diverse; one represented flutter of a T-tail, a second represented flutter of a wing, a third represented flutter of a stabilizer, while a fourth represented flutter of a wing carrying a large external store. All of these were multi-degree-of-freedom systems and, in a rigorous sense, supposedly beyond the applicability of the two-degree-of-freedom analytical development. (No applicable test data could be found for any two-degree-of-freedom configuration.) The comparisons show that in a practical sense, however, the technique can be applied successfully far beyond its theoretical limitations. In further support of the versatility of the technique, detailed configuration information was either not known or, if known, it was not used; only measured frequency and decay data were employed.

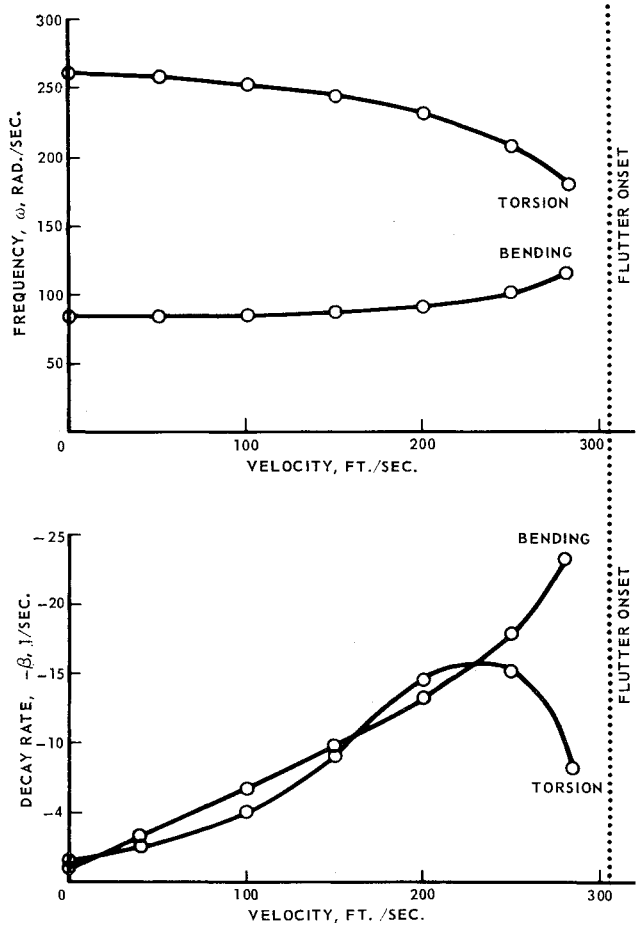

Fig. 6 T-tail flutter model: measured frequency and decay data.

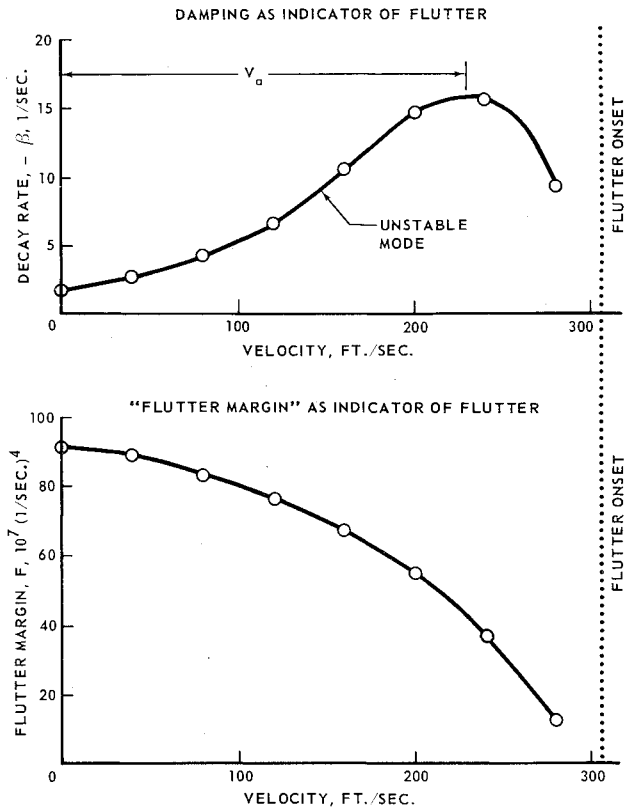

Fig. 7 T-tail flutter model: flutter margin as indication of flutter stability remaining at any airspeed.

T-Tail Flutter Model

The frequency and decay data presented in Fig. 6 were obtained in the course of wind-tunnel tests of a T-tail flutter model. The tests were terminated just short of impending flutter (in the neighborhood of 305 fps) to avoid model damage. We shall check two aspects of the technique here, namely, 1) the validity of the flutter margin as a measure of the flutter stability remaining at any selected speed, and 2) the validity of the prediction technique for anticipating the flutter.

For checking the validity of the flutter margin as an indicator of flutter stability, we shall utilize the full range of the measured frequency and decay data from zero airspeed to just short of 300 fps. The flutter margin, calculated from Eq. (7) with the measured data from Fig. 6, is shown plotted in the lower half of Fig. 7. The continuous erosion of flutter

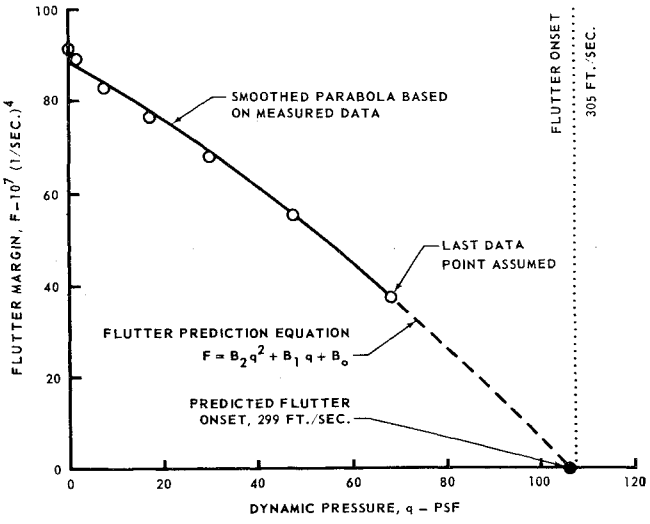

Fig. 8 T-tail flutter model: prediction of flutter onset from measured data at subcritical speeds.

stability margin is clearly evident even at the very low speeds, and it is further seen that this parameter provides early warning of the approaching flutter. To further highlight the value in using this flutter margin in flight flutter test programs, the decay data for the unstable mode of Fig. 6 is replotted directly above the flutter margin. This decay data, in itself, is quite misleading and seemingly appears to indicate increasing stability up to about 225 fps; no warning of the approach to flutter is evident until after this speed.

In demonstrating the prediction aspect of the technique, we shall assume that wind tunnel testing has progressed only to about two-thirds the dynamic pressure of flutter onset. The corresponding flutter margins, plotted against dynamic pressure, are shown as the open circles in Fig. 8, and a parabolic curve shown as a solid line is faired between these data points. Three points on this curve (two at the extremities and one in the middle) were used to evaluate the coefficients B_2, B_1, and B_0 in the flutter prediction equation

$$F = B_2q^2 + B_1q + B_0$$

Having thus evaluated the coefficients, the parabola was continued out beyond the last data point as the dashed extension to yield the predicted flutter onset shown by the solid circle. This corresponds to a predicted flutter onset

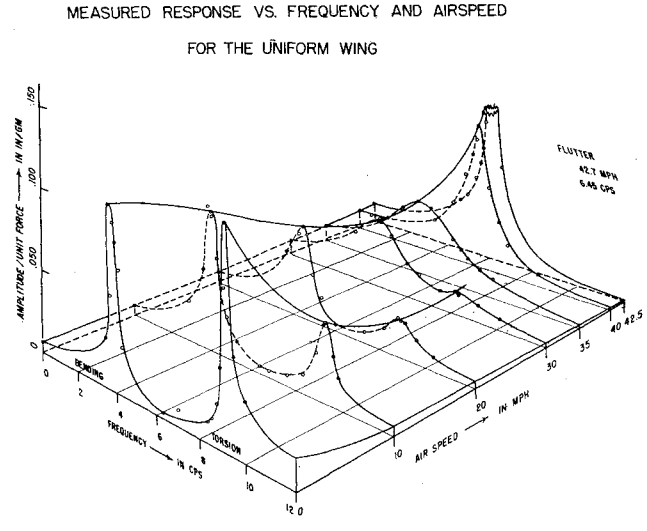

Fig. 9 Flutter model wing: response measured during wind-tunnel flutter tests.

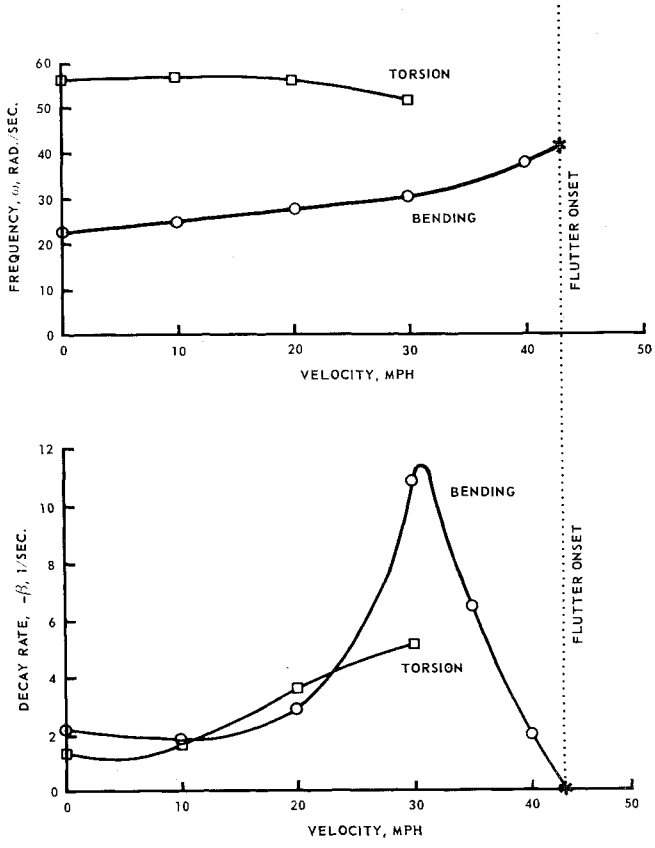

Fig. 10 Flutter model wing: measured frequency and decay data.

speed of 299 fps which compares well with the flutter speed of about 305 fps approached in the wind-tunnel tests.

Wing Flutter Model

The data in Fig. 9 was reproduced from Ref. 1 and represents response data measured during low-speed wind-tunnel tests of a uniform, rectangular flutter model wing. This data is replotted in Fig. 10 where the decay rates shown were computed from the widths of the resonance peaks in Fig. 9. Using these measured data, we shall again check the validity of the two phases of the over-all technique, namely, the use of the flutter margin and the flutter prediction equation.

The flutter margins were computed from Eq. (7) using the measured data shown in Fig. 10 and are shown plotted against velocity in the lower half of Fig. 11. [The flutter margin as expressed in Eq. (7) automatically becomes zero when one of the decay rates becomes zero, regardless of the values for the corresponding frequencies or other decay rate.] As in the previous case for the T-tail, it is again seen that the flutter margin provides early indications of the approaching flutter in direct contrast to the misleading damping trend taken from Fig. 10 and replotted in the upper half of Fig. 11.

In checking the prediction phase of the technique, let it be assumed that the wind-tunnel tests have progressed only to 30 mph, the frequency and decay measurements having been taken at 0, 10, 20, and 30 mph, as shown in Figs. 9 and 10. The flutter margins corresponding to these data are shown as the open circles in Fig. 12, where the margins are plotted against dynamic pressure. As in the previous case, a parabolic curve, shown solid, is faired between the data points. The coefficients B_2, B_1, and B_0 in the flutter prediction equation were evaluated using three points on this curve, one at each extremity and one in the middle. Having evaluated these coefficients, the parabola was continued out beyond the last data point as the dashed extension to yield the predicted

flutter onset speed of 44 mph comparing favorably with the measured flutter speed of 42.7 mph.

Flight Test of Fighter-Type Aircraft

Frequency and decay data measured in the course of flight flutter testing of a fighter-type aircraft are presented in Fig. 13. In this particular situation, stabilizer flutter was encountered at 520 knots. We shall once again check the validity of the two phases of the over-all technique, i.e., use of the flutter margin and the flutter prediction equation.

For checking the validity of the flutter margin as an indicator of flutter stability, the full range of frequency and decay data up to 500 knots is used. Proceeding as in the previous cases, the flutter margin computed from this data is shown plotted against velocity in the lower half of Fig. 14. Here too, we see clear indications of the smooth, continuous erosion of flutter stability and the unmistakable warnings of the approaching flutter. The damping data from the previous figure is shown replotted in the upper part of Fig. 14 for contrast.

For checking the validity of the flutter prediction phase, we shall assume that flight testing has progressed only to about 360 knots, and, consequently, frequency and decay data for the higher speeds are not available. On this basis, only those points shown by the open circles in Fig. 15 can be obtained. Proceeding in much the same manner as in the previous case, we evaluate the coefficients B_2, B_1, and B_0 in the flutter prediction equation from the solid curve faired through the data points. Having evaluated the coefficients, the parabola was continued out beyond the last data point to yield the predicted flutter onset shown by the solid circle which corresponds to an airspeed of 540 knots. This compares well with the flutter speed of 520 knots actually encountered.

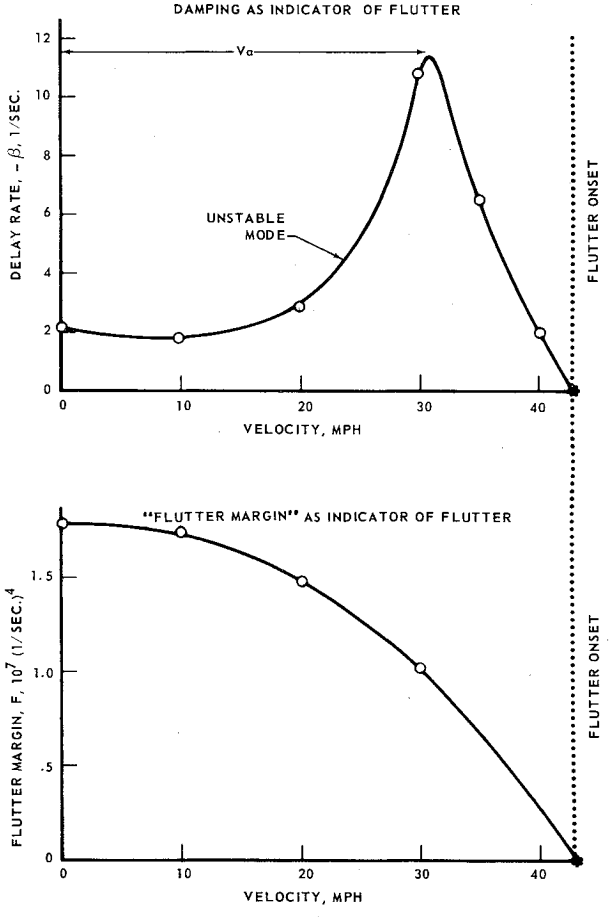

Fig. 11 Flutter model wing: flutter margin as indication of flutter stability remaining at any airspeed.

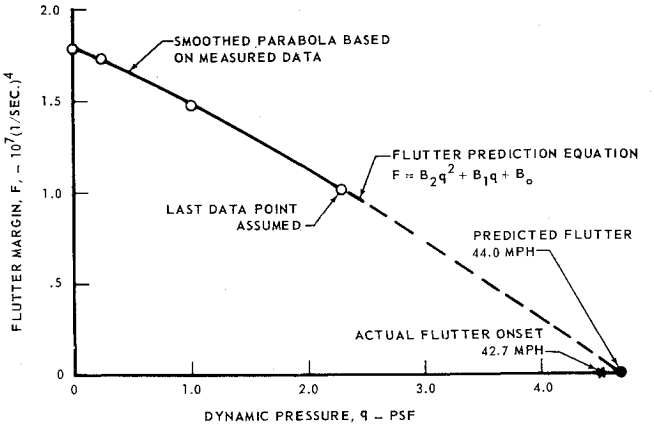

Fig. 12 Flutter model wing: prediction of flutter onset from measured data at subcritical speeds.

At the higher speeds in this example, some compressibility effects were probably present. However, lacking sufficient information to account for this, the compressibility effects were entirely disregarded.

Some Practical Considerations

General

Although experience with this new technique has not yet been extensive, a sufficient familiarity has been attained to permit some pertinent remarks regarding the practical application of the technique for flight flutter testing. In some instances, definite suggestions can be made to help assure a successful test program with this technique. In other instances, the limited familiarity is sufficient to point out some possible difficulties but insufficient at this time to suggest all the answers. Over all, however, the technique, even in its present developmental stage, can be applied with good reliability for a broad range of practical flight flutter test programs.

The over-all flutter prediction technique proposed herein divides itself naturally into two distinct phases, each of which can be handled separately. The first phase involves computation of the flutter margin from frequency and decay data measured up to the last test speed and plotting it against the $C_{L_\alpha}q$ (or frequently just q) corresponding to this data.

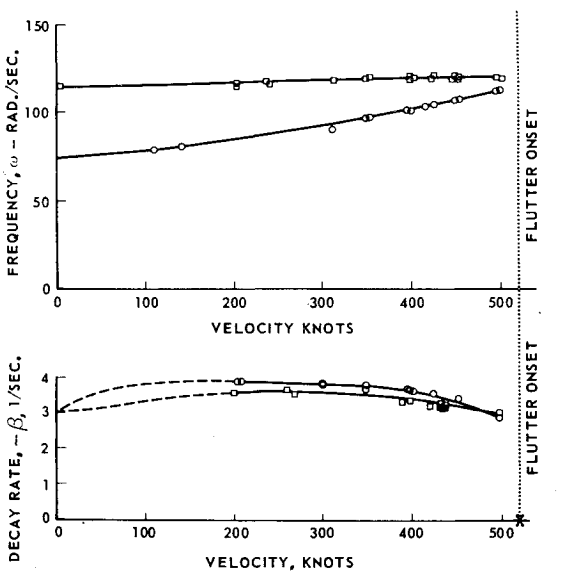

Fig. 13 Stabilizer flutter: measured data from flight test of fighter-type aircraft.

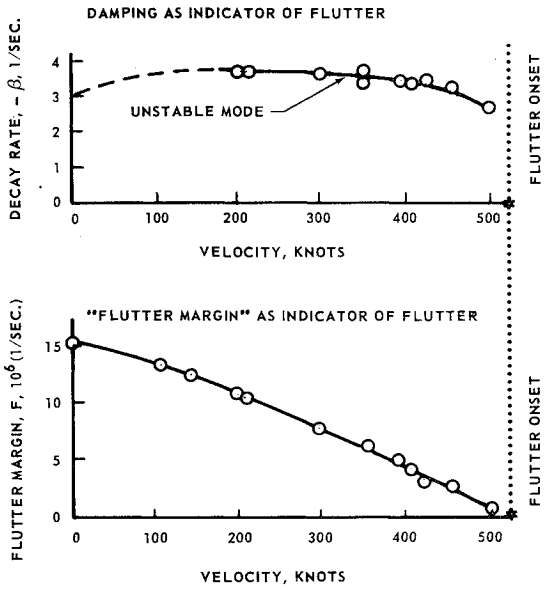

Fig. 14 Stabilizer flutter: flutter margin as indication of flutter stability remaining at any airspeed.

The second phase deals with the aspect of predicting the manner in which the system flutter margin will vary at test speeds not yet encountered through the use of the flutter prediction equation. In practical application to flight flutter testing, the over-all prediction technique can be employed, or if desired, only the first phase. Much valuable information about the system stability is contained within the first phase alone as demonstrated in the previous section. It is subject to fewer restrictions than the second phase, and it can still be used as a reliable indicator of flutter stability in many situations where the validity of the over-all technique may be in question.

Considerations Applicable to the First Phase

Since the flutter margin is computed in direct fashion from measured frequency and decay data, its accuracy is dependent to a large degree upon the accuracy of these measured data. Past experience in flight flutter testing has clearly indicated that reliable measurements of decay are difficult to achieve, even with elaborate techniques, whereas little difficulty has been encountered in obtaining reasonable frequency measurements. The need for accurate decay data, however, has been minimized by the form of Eq. (7) for calculation of the flutter margin. As a matter of fact, considerable scatter in decay data would have correspondingly little effect on the flutter margin.

The validity of the flutter margin, as defined in Eq. (7), as a true indication of existing flutter stability is subject to only one restriction, i.e., that flutter of the specific configuration being investigated result from interaction between the two predominant modes of the system. This imposes no significant limitation, since the preponderance of flutter cases falls within this classification. In a practical sense, prior theoretical studies will most likely precede flight flutter testing, and the validity of the flutter margin can be judged from those studies.

Considerations Applicable to the Second Phase

The prediction phase of the over-all technique requires the evaluation of three coefficients in the quadratic expression relating the dependence of the flutter margin upon $C_{L_\alpha}q$. A reliable flutter prediction equation depends upon the accuracy with which these coefficients are determined. The flutter prediction phase is not overly sensitive to the accuracy in

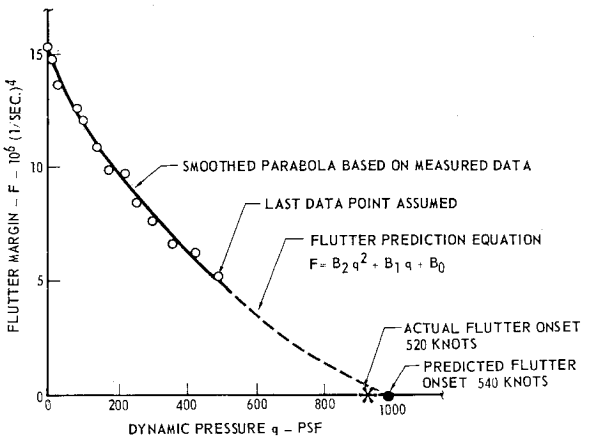

Fig. 15 Stabilizer flutter: prediction of flutter onset from measured data at subcritical speeds.

determining the coefficients of the linear or constant term in the flutter prediction equation, but it is highly sensitive to the coefficient of the quadratic term which reflects the curvature in the flutter margin plot. For instance, consider Fig. 16, which is applicable to the T-tail flutter model considered earlier. At that time, we assumed test data was available up to about two-thirds of the flutter dynamic pressure for demonstrating the applicability of the flutter prediction aspect. (See Fig. 8.) This is redrawn again in Fig. 16. Now, however, assume that test data was available only out to about one-half the flutter dynamic pressure or, more precisely, to the data point shown at a dynamic pressure of 48 psf. If only the six data points shown up to this dynamic pressure were available, the curve faired through these might easily have been drawn with the upward curvature shown as against the downward curvature previously used when we included the next data point. The coefficients B_1 and B_0 in the flutter prediction equation, $F = B_2q^2 + B_1q + B_0$, are not significantly affected whether we use only six data points or seven. However B_2, or really the influence of B_2 in defining the prediction curve, is significantly affected as indicated. Within the limits of the mutually measured data points, both curves lie rather close to each other; they depart considerably only when extended beyond the last data points. This does not imply that the technique is incorrect. It does, though, indicate an area of sensitivity in the application of the prediction technique. This diffi-

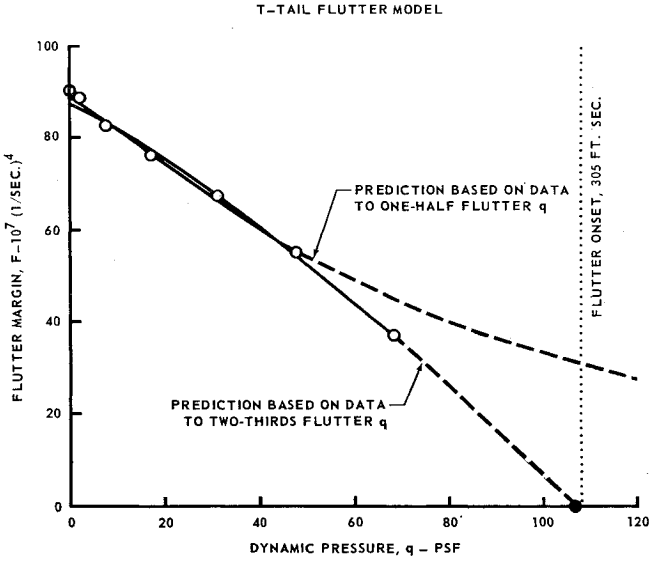

Fig. 16 Sensitivity of flutter prediction technique for insufficient data points.

culty can be circumvented by taking data points at closer intervals to define a more precise curve, or, preferably, by re-checking the flutter prediction as additional data is acquired with increasing dynamic pressure.

Aside from sensitivity, the validity of the flutter prediction equation is subject to somewhat greater restrictions than the flutter margin in that compressibility effects can tend to alter the prediction equation from the quadratic form developed earlier in this paper. In the theoretical development of the prediction technique, it was assumed that the location of the aerodynamic center remained fixed and could be lumped in with the other configuration constants. Thus, shifts in aerodynamic center which occur as airspeed traverses the transonic region would require some modification to the form of the prediction equation in this region. The quadratic form again becomes valid for all practical purposes above the transonic range (where the sizable aerodynamic center shifts occur), and the technique can be used again in the supersonic region. The modifications required to obtain a valid flutter prediction equation in the transonic range have not been undertaken to date. Some additional comments on the influence of the aerodynamic center shift are covered in Appendix B on refinements.

Acquisition of Test Data

An important problem arises in connection with acquiring the flight data needed for the application of the technique. Although the data requirements, namely, natural frequencies and decay rates, are no more extensive than those normally attained in previous flight flutter test techniques, the reliable acquisition of this information can pose some difficulty. This is demonstrated in Fig. 9, where the data shown represents the response to resonance excitation. Note that, as the flutter speed is approached, the unstable mode tends to show a well-defined resonance peak, while at the same time the other mode tends to lose its identity with any peak response. As a matter of fact at 35 mph no peak is discernible at all. Thus the needed frequency and decay data for this mode would not be available at speeds of 35 mph and above, at least not by the usual method of associating resonance with peak response and damping with the width of the peak. Even though this behavior in resonance response is typical, the stable mode does not generally "lose" its identity until the flutter speed is closely approached, and sufficient frequency and decay data would have been taken to allow for reasonably reliable application of the flutter margin and flutter prediction techniques. This can be seen by referring to Figs. 11 and 12, which are based on this data.

Another possible way out of this difficulty lies in the relation that exists between the shape of the over-all resonance response curve for systems possessing more than one-degree-of-freedom and the associated frequencies and dampings. It is not necessary that a peak exist for each natural frequency, particularly if damping is large. At any rate we shall not pursue this further in this paper.

Conclusions

The more significant conclusions that may be drawn are listed below.

1) The usual decay rates obtained during flight flutter tests below the critical flutter speed have, in themselves, only a remote relation to the processes leading to flutter and are hardly the guide to follow for predicting the progress toward a fluttering condition. The decay rates have significance only when they change from positive to negative.

2) A reliable and simple technique for predicting flutter onset speed based on measured in-flight frequency and decay data at subcritical speeds is feasible. The technique is based on the use of a flutter margin which is fundamentally indicative of the stability processes going on within the system. The variation of this margin with airspeed clearly shows the progress of stability degradation all the way from zero airspeed on up. It varies smoothly with airspeed and is not subject to sudden and unexpected reversals such as those that occur with decay rates, particularly in cases of explosive flutter. The flutter severity to be expected is also indicated.

3) The concepts presented in this paper set forth a basic foundation upon which an entirely new and practical philosophy of flight flutter testing can be built. Further refinements for extending its range of applicability and degree of reliability are suggested and could be achieved without undue difficulty.

Appendix A: Details of the Analytical Development

General

The detailed derivation of the equations which lead to the flight flutter criteria are developed herein. This appendix is divided into two subsequent sections. In the first, the equations of motion for the two-degree-of-freedom bending/torsion airfoil are derived in a form suitable for subsequent extraction of the criteria and concludes with the differential equation describing the system motion. The second section starts with this differential equation, and from subtleties contained therein proceeds to the development of the equations needed for the criteria.

The bending/torsion idealization has been used in developing the equations of motion to enhance retention of physical significance. For the purpose at hand, only the form of the final differential equation has any significance in the ultimate development of the criteria. A generalized two-degree-of-freedom idealization and development leads to the same form of the differential equation.

Equations of Motion

The two-degree-of-freedom bending/torsion idealization is shown schematically in Fig. 3. All the physical quantities to be used represent weighted spanwise averages. The corresponding free body diagram is shown in Fig. 4.

Summing forces, positive down,

$$m\ddot{h} + k_h h - (k_h x)\alpha + L = 0 \tag{A1}$$

Summing torques, positive nose up,

$$I_c\ddot{\alpha} + (k_\alpha + k_h x^2)\alpha - (k_h x)h - M_c = 0 \tag{A2}$$

Aerodynamic forces referred to the center of gravity of the airfoil are of the form

$$\begin{aligned} L &= C_{L_\alpha} q \left[a_1\alpha + a_2\left(\frac{\dot{h}}{V}\right) + a_3\left(\frac{\dot{\alpha}}{V}\right)\right] \\ M_c &= C_{L_\alpha} q \left[b_1 a + b_2\left(\frac{\dot{h}}{V}\right) + b_3\left(\frac{\dot{\alpha}}{V}\right)\right] \end{aligned} \tag{A3}$$

Substituting the expression for the aerodynamics, Eq. (A3), into the equations of motion,

$$m\ddot{h} + C_{L\alpha} q a_2\left(\frac{\dot{h}}{V}\right) + k_h h + C_{L_\alpha} q a_3\left(\frac{\dot{\alpha}}{V}\right) + (C_{L_\alpha} q a_1 - k_h x)\alpha = 0 \tag{A4}$$

$$I_c\ddot{\alpha} - C_{L_\alpha} q b_3\left(\frac{\dot{\alpha}}{V}\right) + (k_\alpha + k_h x^2 - C_{L_\alpha} q b_1)\alpha - C_{L_\alpha} q b_2\left(\frac{\dot{h}}{V}\right) - (k_h x)h = 0 \tag{A5}$$

Writing these equations in operational form with P repre-

senting d/dt and performing some algebraic manipulations, they can be written as

$$\left\{P^2 + \left(\frac{a_2}{m}\right)\left(\frac{C_{L_\alpha}q}{V}\right)P + \left(\frac{k_h}{m}\right)\right\}h + \left\{\left(\frac{a_3}{m}\right)\left(\frac{C_{L_\alpha}q}{V}\right)P + \left(\frac{a_1}{m}\right)(C_{L_\alpha}q) - \left(\frac{k_h x}{m}\right)\right\}\alpha = 0 \quad \text{(A6)}$$

$$-\left\{\left(\frac{b_2}{I_c}\right)\left(\frac{C_{L_\alpha}q}{V}\right)P + \left(\frac{k_h x}{I_c}\right)\right\}h + \left\{P^2 - \left(\frac{b_3}{I_c}\right)\left(\frac{C_{L_\alpha}q}{V}\right)P + \left[\left(\frac{k_\alpha + k_h x^2}{I_c}\right) - \left(\frac{b_1}{I_c}\right)C_{L_\alpha}q\right]\right\}\alpha = 0 \quad \text{(A7)}$$

These two simultaneous differential equations in the unknowns h and α can be reduced to a single differential equation in either of the unknowns using straightforward operational techniques. If the unknown h is eliminated, we obtain the differential equation for α,

$$(P^4 + A_3P^3 + A_2P^2 + A_1P + A_0)\alpha = 0 \quad \text{(A8)}$$

The exact expressions for the coefficients A_0–A_3 are unimportant for our purpose; only the form or composition are pertinent. The coefficients A_0–A_3 take the form

$$\begin{aligned} A_0 &= K_{01}(C_{L_\alpha}q) + K_{02} \\ A_1 &= K_{11}\frac{(C_{L_\alpha}q)^2}{V} + K_{12}\left(\frac{C_{L_\alpha}q}{V}\right) \\ A_2 &= K_{21}\left(\frac{C_{L_\alpha}q}{V}\right)^2 + K_{22}C_{L_\alpha}q + K_{23} \\ A_3 &= K_{31}\left(\frac{C_{L_\alpha}q}{V}\right) \end{aligned} \quad \text{(A9)}$$

where the K's represent configuration constants; they are employed to distinguish between the dependence of the A's on configuration from the dependence on airspeed. The specific expressions for the K's are given below:

$$\begin{aligned} K_{01} &= \frac{k_h(a_1x - b_1)}{mI_c} \\ K_{02} &= \frac{k_h k_\alpha}{mI_c} \\ K_{11} &= \frac{a_1b_2 - a_2b_1}{mI_c} \\ K_{12} &= \frac{a_2(k_\alpha + k_h x^2) + k_h x(a_3 - b_2) - k_h b_3}{mI_c} \\ K_{21} &= \frac{a_2b_3 + a_3b_2}{mI_c} \qquad K_{22} = \frac{-b_1}{I_c} \\ K_{23} &= \left(\frac{k_h}{m}\right) + \frac{k_\alpha + k_h x^2}{I_c} \\ K_{31} &= \frac{a_2}{m} - \frac{b_3}{I_c} \end{aligned} \quad \text{(A10)}$$

Flight Flutter Criteria

The resulting pitch motion α is obtained from solution of Eq. (A8). Since the coefficients A_0–A_3 depend on airspeed as well as on configuration, it is to be expected that the resulting pitch motion will also vary with speed. At any selected speed, however, Eq. (A8) represents a linear differential equation with constant coefficients whose solution is of the form

$$\alpha = \sum_{j=1}^{j=4} \alpha_{0j}e^{s_j t}$$

where α_{0j} are arbitrary integration constants and s_j are the four roots of the corresponding characteristic equation

$$s^4 + A_3s^3 + A_2s^2 + A_1s + A_0 = 0 \quad \text{(A11)}$$

The roots s_j may be expressed in the complex form

$$s_j = \beta_j + i\omega_j$$

and, since the coefficients of the characteristic equation are all real, these must occur in the conjugate pairs

$$s_{1,2} = \beta_1 \pm i\omega_1 \qquad s_{3,4} = \beta_2 \pm i\omega_2 \quad \text{(A12)}$$

Thus the characteristic equation may be written in the alternate form

$$[s - (\beta_1 + i\omega_1)][s - (\beta_1 - i\omega_1)]$$
$$[s - (\beta_2 + i\omega_2)][s - (\beta_2 - i\omega_2)] = 0$$

Expanding this out and comparing like coefficients with Eq. (A11), we have

$$\left.\begin{aligned} A_3 &= -2(\beta_1 + \beta_2) \\ A_2 &= (\beta_1^2 + \omega_1^2) + (\beta_2^2 + \omega_2^2) + 4\beta_1\beta_2 \\ A_1 &= -2[\beta_1(\beta_2^2 + \omega_2^2) + \beta_2(\beta_1^2 + \omega_1^2)] \\ A_0 &= (\beta_1^2 + \omega_1^2)(\beta_2^2 + \omega_2^2) \end{aligned}\right\} \quad \text{(A13)}$$

The stability boundary is the point at which one of the real parts β of the solution becomes zero. Setting one of the β's equal to zero in Eqs. (A13) gives the following familiar relationship between the coefficients of the characteristic equation at the stability boundary (flutter onset):

$$A_2(A_1/A_3) - (A_1/A_3)^2 - A_0 = 0 \quad \text{(A14)}$$

For subsequent use, this is written in the preferable form

$$\left[\left(\frac{A_2}{2}\right)^2 - A_0\right] - \left[\frac{A_2}{2} - \frac{A_1}{A_3}\right]^2 = 0 \quad \text{(A15)}$$

It will be convenient to define a variable function of $C_{L_\alpha}q$ by the relation

$$F = F(C_{L_\alpha}q) = \left[\left(\frac{A_2}{2}\right)^2 - A_0\right] - \left[\frac{A_2}{2} - \frac{A_1}{A_3}\right]^2 \quad \text{(A16)}$$

which varies with $C_{L_\alpha}q$ because of the dependence of the A's on $C_{L_\alpha}q$, Eq. (A9). At flutter onset, i.e., when $(C_{L_\alpha}q)$ is equal to $(C_{L_\alpha}q)_f$,

$$F_f = F(C_{L_\alpha}q)_f = 0 \quad \text{(A17)}$$

by virtue of Eq. (A15). Otherwise, $F(C_{L_\alpha}q)$ will be nonzero.

A more direct indication of how F varies with $(C_{L_\alpha}q)$ is readily obtained by introducing the A's defined by Eq. (A9) into Eq. (A16). This results in an expression of the form

$$F = B_2(C_{L_\alpha}q)^2 + B_1(C_{L_\alpha}q) + B_0 \quad \text{(A18)}$$

where the coefficients are

$$\left.\begin{aligned} B_2 &= \frac{K_{11}}{K_{31}}\left(\frac{K_{11}}{K_{31}} + K_{22}\right) + \frac{\rho C_{L_\alpha}}{2}\left(\frac{K_{11}K_{21}}{K_{31}}\right) \\ B_1 &= \left(\frac{1}{K_{31}}\right)\left(K_{12}K_{22} + K_{11}K_{23} - 2\frac{K_{11}K_{12}}{K_{31}}\right) - K_{01} + \frac{\rho C_{L_\alpha}}{2}\left(\frac{K_{12}K_{21}}{K_{31}}\right) \\ B_0 &= \frac{K_{12}}{K_{31}}\left(K_{23} - \frac{K_{12}}{K_{31}}\right) - K_{02} \end{aligned}\right\} \quad \text{(A19)}$$

Equation (A18), expressing a parabolic variation of F with $(C_{L_\alpha}q)$, will be referred to as the "flutter prediction equa-

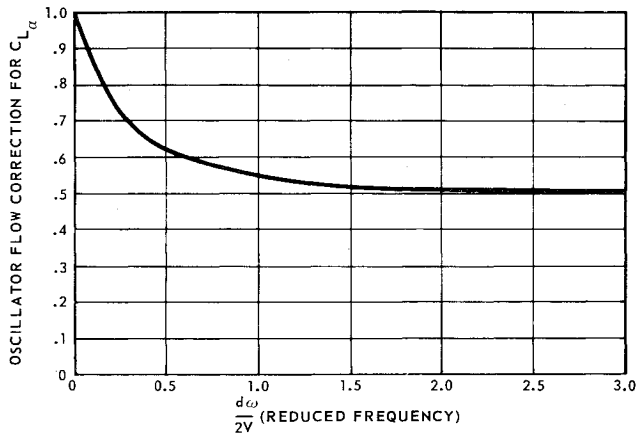

Fig. 17 Oscillatory flow correction for $C_{L\alpha}$.

tion" whereas F itself will be referred to as the "flutter margin." The complex dependence of the B coefficients upon specific configuration parameters is of no concern for the purpose at hand, as will be seen in the subsequent development. The B coefficients need not be computed from design details of the specific configuration being flight tested. These may be evaluated more readily (and, incidentally, more reliably) in the early stages of flight flutter testing at the lower speeds. The manner in which this is accomplished is developed in the next paragraph.

Let us return again to Eq. (A16). In the previous paragraph we replaced A_0–A_3 by their equivalents in terms of configurations constants and $(C_{L_\alpha}q)$, as reflected by Eq. (A9), in order to arrive at the parabolic variation of F with $(C_{L_\alpha}q)$. But the flutter margin F can also be expressed in terms of frequencies and decay rates that could be measured in flight. The relation between F and such measured flight data can be readily obtained by substituting into Eq. (A16) the alternate expressions for A_0–A_3, Eq. (A13), thus introducing the dependence upon frequencies and decay rates. The expression for the flutter margin then becomes

$$F = \left[\left(\frac{\omega_2^2 - \omega_1^2}{2}\right) + \left(\frac{\beta_2^2 - \beta_1^2}{2}\right)\right]^2 + 4\beta_1\beta_2\left[\left(\frac{\omega_2^2 + \omega_1^2}{2}\right) + 2\left(\frac{\beta_1 + \beta_2}{2}\right)^2\right] - \left[\left(\frac{\beta_2 - \beta_1}{\beta_2 + \beta_1}\right)\left(\frac{\omega_2^2 - \omega_1^2}{2}\right) + 2\left(\frac{\beta_1 + \beta_2}{2}\right)^2\right]^2 \quad \text{(A20)}$$

With further manipulating, this can be expressed in more compact form as

$$F = \left[1 - \left(\frac{\beta_2 - \beta_1}{\beta_2 + \beta_1}\right)^2\right]\left\{\left(\frac{\omega_2^2 - \omega_1^2}{2}\right)^2 + (\beta_1 + \beta_2)^2\left[\left(\frac{\omega_2^2 + \omega_1^2}{2}\right) + \left(\frac{\beta_1 + \beta_2}{2}\right)^2\right]\right\} \quad \text{(A21)}$$

This latter form, however, is overly sensitive to errors in decay measurements, and consequently will be bypassed in favor of Eq. (A20). At flutter onset, either β_1 or β_2 is zero, and it can be seen from Eq. (A20) or (A21) that F also becomes zero at flutter onset as indeed it should.

Equations (A18) and (A20) form the basis of the flight flutter prediction technique used in this paper.

Appendix B: Refinements to the Basic Approach

As indicated earlier in this paper, some detailed effects had been purposely avoided in the interest of clarity in presenting the basic concepts of a new flight flutter testing technique. This appendix discusses some detailed effects previously avoided.

Oscillatory Flow Correction of C_{L_α}

The parabolic relationship developed between the flutter margin F and the product $(C_{L_\alpha}q)$ implies that F can vary with a change in C_L as well as q. Consequently, the product $(C_L\ q)$ must account for the possibility that C_L may vary in the flight test program as well as q. The variation of C_{L_α} due to steady compressible aerodynamic effects can be accounted for in a reasonably straightforward manner employing either steady flow theory or experimental data, or both. A rather simple, but effective method of accounting for oscillatory flow effects on C_L was suggested by Pines in Ref. 2. This correction is shown plotted in Fig. 17 as a function of the reduced frequency $d\omega/2V$ where d would represent the averaged airfoil chord. The correction simply amounts to multiplying the steady flow C_L by the ordinate for the applicable reduced frequency. Normally this correction has only a slight effect on the results.

Mechanical Damping Effects

The equations of motion, Eq. (1), used in developing the basic approach did not include any terms accounting for mechanical damping in the system. This has no effect on the determination of the flutter margins from measured fre-

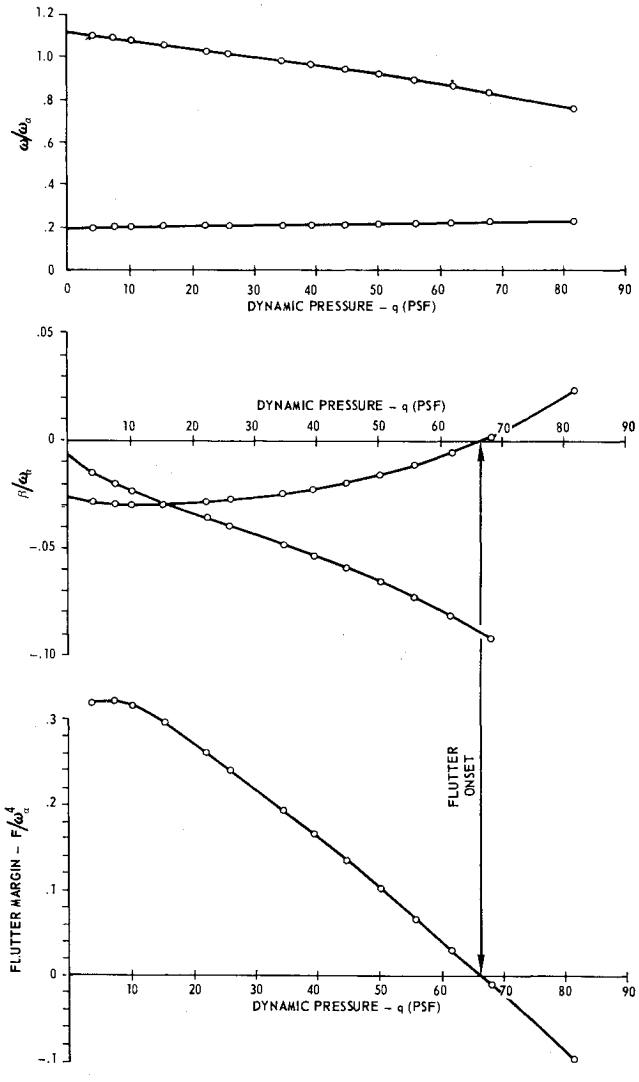

Fig. 18 Effect of significant mechanical damping.

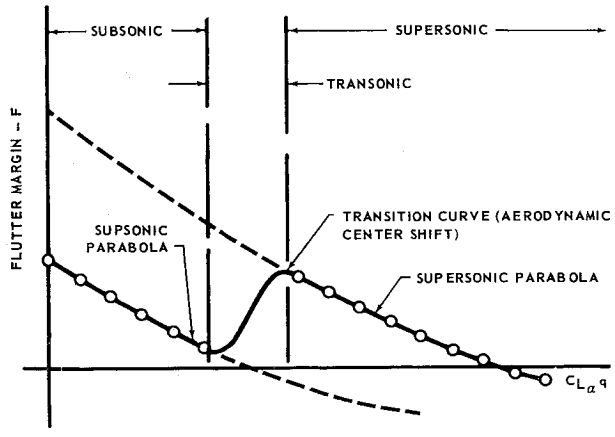

Fig. 19 Variation of flutter margin in subsonic, transonic, and supersonic flight regimes.

quencies and decays, Eq. (7), or on the validity of the flutter margin as a reliable indication of flutter stability for the corresponding speed. It does not affect the idea of a flutter prediction equation; it merely changes it from a quadratic expression in dynamic pressure to a sixth-order expression in velocity. These effects are indicated in Fig. 18 for a hypothetical theoretical configuration possessing a significant amount of mechanical damping. The theoretical frequencies and decays for this configuration are shown plotted against q in the two upper graphs of Fig. 18. The flutter margins computed from these data via Eq. (7) are shown in the lower graph. It is seen that the flutter margin, even in this case with considerable mechanical damping, is still a reliable guide for indicating the progress toward flutter. The quadratic form of the flutter prediction equation, derived on the basis of no mechanical damping, would not be too good for this case.

A prediction equation of sixth-order in velocity would show better agreement here, although this is not actually shown in the figure.

Compressible Flow Aerodynamic Effects

Compressible flow aerodynamic effects on C_{L_α} and aerodynamic center can have a pronounced influence on the application of the flight flutter approach presented herein. The method of accounting for compressibility effects on C_{L_α} is straightforward and has already been indicated elsewhere in this paper.

Compressibility effects on aerodynamic center, however, have a less obvious influence on the application of the technique. In the analytical development of the basic technique, it was assumed in Eq. (2) for the aerodynamic moment that the coefficients b_1–b_3 were constants. This assumption permits the subsequent development of the quadratic expression, Eq. (8), for the variation of flutter margin with $C_{L_\alpha}q$. Sizable aerodynamic center shifts, such as occur in the transonic region, are not compatible with this assumption, and taking account of the corresponding variations in these coefficients would result in a more complex expression for the flutter margin variation. In a practical sense the quadratic form of the flutter prediction equation is satisfactory in the subsonic and supersonic regions but is grossly inadequate in the transonic region. Aerodynamic center shifts have no influence on Eq. (7) for calculating the flutter margin from flight measurements of frequencies and decays.

Figure 19 illustrates a typical variation of flutter margin with $C_{L_\alpha}q$ for a hypothetical flight program penetrating deeply into the supersonic region. Below the transonic region the variation would follow the quadratic flutter prediction equation developed in the basic technique; in the supersonic region, where aerodynamic center shifts are small, the variation would again be essentially quadratic. In this region the quadratic flutter prediction equation can again be employed for anticipating the approaching flutter. The technique is similar to that employed elsewhere in this paper for the subsonic cases except that only the supersonic data points are to be used for evaluating the coefficients B_2, B_1, and B_0.

The prediction phase of the technique for configurations which may flutter in the transonic region has not as yet been

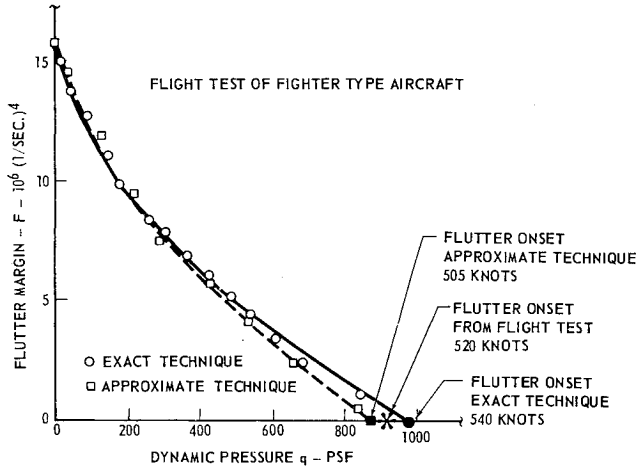

Fig. 20 Comparison between approximate and exact techniques.

developed. Although the applicable flutter prediction equation would undoubtedly be more complex, the practical development of such an equation should be within the realm of possibility. It would have to take into account theoretical or experimental information for expressing the transonic variation of aerodynamic center.

Appendix C: Approximate Flutter Test Criteria

In view of the fact that past flight flutter test programs have for the most part emphasized the importance of the decay or damping aspects, it might appear paradoxical that the behavior of the system frequencies is a more direct indication of the stability processes going on within the system than the damping behavior. There is a certain logic behind this statement, such as that in Ref. 3, but we shall not dwell on the details of this logic here. This logic leads to the approximate flutter prediction equation

$$[(\omega_2^2 - \omega_1^2)/2]^2 \cong B_2(C_{L_\alpha}q)^2 + B_1(C_{L_\alpha}q) + B_0 \quad \text{(C1)}$$

Comparing this equation with Eqs. (7) and (8), it is seen that the approximation simply amounts to dropping all terms in the expression for the flutter margin F in Eq. (7) except for the first term $[(\omega_2^2 - \omega_1^2)/2]^2$. That this term is predominant by far can be seen in Fig. 20, where the complete flutter margin based on Eq. (7) is compared with the approximation based on frequencies alone. Although this is shown only for the experimental flight data previously considered, comparisons had been made with other sets of data which also substantiate the validity of the approximation. Thus the frequency expression may be regarded as an approximate flutter margin, i.e.,

$$F \cong [(\omega_2^2 - \omega_1^2)/2]^2 \quad \text{(C2)}$$

The extreme simplicity of Eqs. (C1) and (C2) make them ideal for rapid, on-the-spot monitoring of the progress of a flight

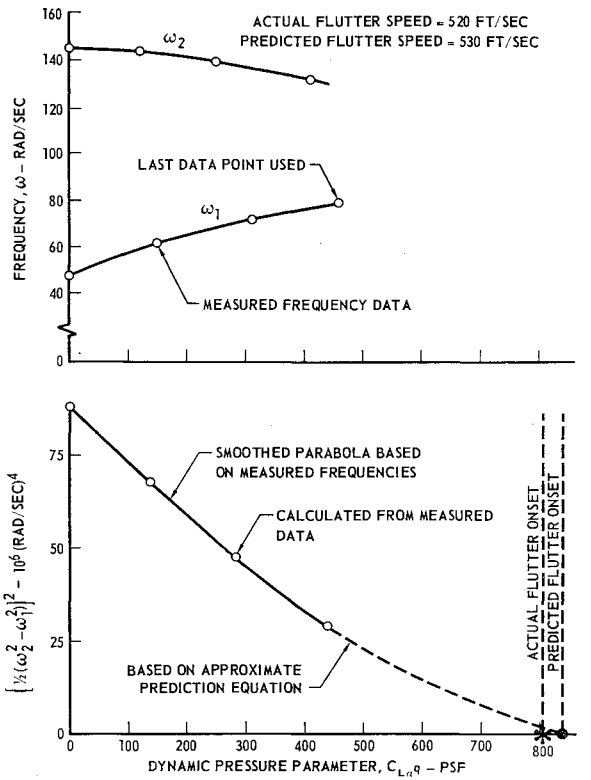

Fig. 21 Flutter model wing with external tank: approximate technique.

flutter test program and can give early indications of the rate of loss of flutter margin with increasing speed.

In Fig. 21 the approximate criterion has been applied to test data taken during wind-tunnel flutter tests of a model wing carrying a large underslung external tank. The circled points were calculated in accordance with the approximation of Eq. (C2) using the measured frequency data up to the last point shown. The analytical extension of this curve, shown dashed, was computed in accordance with the parabolic relation of Eq. (C1) using the previously described technique for determining the coefficients B_2, B_1, and B_0. The predicted flutter speed of 530 fps differs by only 10 fps from the measured model flutter speed. Although the agreement is good here, flutter prediction based on the approximate technique should be used with a degree of caution, since it is known that the damping effects do have some influence on the exact flutter margin. It has been the authors' experience that the accuracy of the approximate technique is somewhat insufficient for configurations prone to mild flutter, good for configurations prone to moderate flutter, and very good (when it counts most) for configurations prone to violent flutter. At any rate, it is recommended at this time that the approximate technique be limited primarily to on-the-spot monitoring of the progress of a flight flutter test program for the purpose of observing loss of flutter margin up to the last measured test point; any prediction, if based on the approximate criterion, should not be extended too far beyond the last previous flight test point. Perhaps its most important role would be in providing a clear-cut early warning of an approaching violent flutter.

References

[1] Smith, R. H. and Schwartz, M. D., "Theoretical and experimental methods of flutter analysis," Massachusetts Institute of Technology, Dept. of Aeronautical Engineering, Navy Bureau of Aeronautics Contract NOa(s) 8790, Vol. 2 (November 15, 1948).

[2] Pines, S., "An elementary explanation of the flutter mechanism," *Proceedings of Dynamics and Aeroelasticity Meeting* (Institute of Aeronautical Sciences, New York, 1958), pp. 52–59.

[3] Zimmerman, N. H., "Elementary static aerodynamics adds significance and scope in flutter analyses," *AIA Symposium Proceedings on Structural Dynamics of High Speed Flight, 1961* (Aerospace Industries Association, Los Angeles, 1961), pp. 28–84